4446–4453 *Nucleic Acids Research, 1998, Vol. 26, No. 19*

Different cleavage specificities of RNases III from *Rhodobacter capsulatus* and *Escherichia coli*

Christian Conrad, Reinhard Rauhut and Gabriele Klug*

Institut für Mikro- und Molekularbiologie der Justus-Liebig-Universität Giessen, Frankfurter Strasse 107, 35392 Giessen, Germany

Received June 2, 1998; Revised and Accepted August 13, 1998

ABSTRACT

23S rRNA in *Rhodobacter capsulatus* shows endoribonuclease III (RNase III)-dependent fragmentation *in vivo* at a unique extra stem–loop extending from position 1271 to 1331. RNase III is a double strand (ds)-specific endoribonuclease. This substrate preference is mediated by a double-stranded RNA binding domain (dsRBD) within the protein. Although a certain degree of double strandedness is a prerequisite, the question arises what structural features exactly make this extra stem–loop an RNase III cleavage site, distinguishing it from the plethora of stem–loops in 23S rRNA? We used RNase III purified from *R.capsulatus* and *Escherichia coli*, respectively, together with well known substrates for *E.coli* RNase III and RNA substrates derived from the special cleavage site in *R.capsulatus* 23S rRNA to study the interaction between the *Rhodobacter* enzyme and the fragmentation site. Although both enzymes are very similar in their amino acid sequence, they exhibit significant differences in binding and cleavage of these *in vitro* substrates.

INTRODUCTION

Ribonucleases (RNases) are key components of the cell, converting mostly inactive RNA precursors into biologically active mature RNA molecules. One of these ribonucleases is endoribonuclease III (RNase III, EC 1.3.24). RNase III cleaves rRNA precursors in bacteria and yeast during maturation of rRNA (1,2). The *Escherichia coli* enzyme participates in precursor rRNA trimming, but is also involved in other pathways of RNA turnover (3,4). Acting on their respective mRNAs, RNase III directly influences the level of a broad variety of corresponding cellular proteins. In *E.coli* RNase III represents only 0.01% of total cell protein (5) and although the enzyme is not essential for viability (6), its presence and primary sequence are highly conserved in nearly all known bacterial genomes, even in the minimal genome of *Mycoplasma genitalium* (7). In the α purple bacterium *Rhodobacter capsulatus* the 23S rRNA is fragmented *in vivo* into 16S and 14S rRNA molecules. As shown previously, this fragmentation is RNase III-dependent (8). In contrast to *E.coli*, *Rhodobacter* 23S rRNA has an extra stem–loop inserted in helix 46 which serves as the RNase III cleavage site. The two resulting rRNA fragments are joined non-covalently *in vivo* to generate a functional 23S rRNA. Fragmentation of rRNA occurs in some other bacteria, for instance in *Salmonella* spp. (9,10), some cyanobacteria (11), *Agrobacterium tumefaciens* (12) and *Rhodobacter sphaeroides* (13), a close relative of *R.capsulatus*. The biological function of rRNA fragmentation still remains unclear (14), although there is some evidence that fragmented rRNA may provide a selective advantage for the bacterium under certain growth conditions (15,16). The amino acid sequence of *R.capsulatus* RNase III closely resembles other bacterial RNase III proteins (17). The processing specificity of RNase III is still poorly understood. This relates to both participants of this particular RNA–protein recognition system. RNase III substrates consist of structured nucleotide stretches with various patterns of intramolecular base pairing but lacking a consensus on the level of the primary sequence. The resulting double helical structure of ~20 bp (approximately two helical turns) contains one or two scissile internucleotide bonds. The deep and narrow major groove of A-form double-stranded (ds)RNA, inaccessible for potential protein contacts, could explain the lack of a consensus sequence. Cleavage is precise, but is not readily predictable from structure or sequence. Recently, the concept of anti-determinants, well known from tRNA recognition (18), has been applied to RNase III substrates. An RNase III cleavage site would thus be defined by the absence of 'disfavoured' sequence motifs (19). On the side of the protein the contribution of the C-terminal dsRNA binding domain (dsRBD) module in creating substrate specificity appears critical. The dsRBD is a ubiquitous protein module present in a widely diverse class of regulatory proteins which bind folded RNAs (20). The module can be present in a protein in multiple copies (21,22). Biological activity in many cases relies only on specific binding without subsequent (nucleolytic) catalysis. In this work we analyse the structural basis for the interaction between *R.capsulatus* RNase III and the fragmentation signal in 23S rRNA.

MATERIALS AND METHODS

Overexpression of *R.capsulatus* $(His)_6$-RNase III in *E.coli*

The *rnc* gene for RNase III of *R.capsulatus* was PCR amplified. A pGEM-3Zf(–) plasmid (Promega) harbouring a 1.7 kb *Pst*I

*To whom correspondence should be addressed. Tel: +49 641 99 35542; Fax: +49 641 99 35549; Email: gabriele.klug@mikro.bio.uni-giessen.de

fragment containing the entire *R.capsulatus rnc* gene (23) was used as template. PCR primers were as follows: *rncPst*Iup, 5′-GAAAGTTGCTGCAGACCTCTCTGC-3′; *rncHin*dIIIdown, 5′-CGAATCAAGCTTGCGTTTCTTCGG-3′ (*Pst*I and *Hin*dIII sites, respectively, are underlined). The resulting product (~700 bp) was purified (Qiaex DNA gel extraction kit; Qiagen) and cloned into the *Pst*I and *Hin*dIII sites of the polylinker of the hexahistidine tag vector pQE-30 (Qiagen). For further characterization the resulting plasmid (pQE-30[*Rc rnc*]) was transformed into *E.coli* JM109 (Stratagene). The correct sequence was confirmed by DNA sequencing. In addition to the N-terminal hexahistidine tag, the cloned RNase III of *R.capsulatus* contains 15 vector-encoded N-terminal amino acids not present in the wild-type RNase III. For protein expression the vector was propagated in *E.coli* M15[pREP4] cells (Qiagen) at 37°C using standard I medium containing ampicillin (200 µg/ml) and kanamycin (25 µg/ml). Overexpression of recombinant RNase III was induced by adding IPTG at a final concentration of 1.5 mM when cells reached an OD_{600} of 0.8. After continued incubation at 37°C for 2 h, the cells were harvested by centrifugation at 5000 *g* and stored at –70°C.

Purification of *R.capsulatus* $(His)_6$-RNase III

All of the following steps were carried out on ice following the protocol for native purification of soluble proteins (Qiagen). An aliquot of 1.4 g induced *E.coli* cells was resuspended in sonication buffer (50 mM NaCl, 50 mM Tris–HCl, pH 7.5, 0.1 mM PMSF). Lysozyme was added at a final concentration of 1 mg/ml. The suspension was incubated for 30 min on ice and subsequently sonicated five times using a Sonopuls GM 70 sonicator (Bandelin). A sample of 7 ml Ni-NTA–agarose was prepared and equilibrated essentially following the manufacturer's protocol (Qiagen). The His-tagged protein was bound to the agarose in a batch procedure for 2 h with vigorous shaking on ice. The material was packed into a column (1.6 cm diameter) and washed with sonication buffer at a flow rate of 0.5 ml/min until the UV baseline was reached. To remove contaminating proteins the column was then washed extensively with sonication buffer containing 20 mM imidazole. The recombinant protein was eluted with a gradient of 0–500 mM imidazole in sonication buffer (90 min, 0.5 ml/min) using a GradiFrac® chromatography system (Pharmacia). Fractions of 1 ml were collected and kept at 4°C or at –70°C for long-term storage. Prior to use during enzymatic assays the RNase III fractions were dialysed in a cold room against dialysis buffer (50 mM Tris–HCl, pH 7.5, 50 mM NaCl, 0.01% sodium azide, 1 mM DTT). A mock purification under the same conditions was performed with *E.coli* M15 cells expressing the pQE30 vector alone.

Purification of *E.coli* RNase III

Escherichia coli RNase III was purified from the overexpressing *E.coli* strain HMS174(DE3)/pET-11a(*mc*) as previously described (24).

Construction of DNA templates for *in vitro* transcription of RNAs

The DNA template for *in vitro* transcription of the *Rc* mini RNA was constructed by PCR using genomic DNA of *R.capsulatus* as template and the following primers: *Rc*mini23S sense, 5′-GGGGGGAATTCTAATACGACTCACTATAGGTTCTGTGATATAGCACCGCCCGACTTTAGC-3′ (60 nt, *Eco*RI site underlined); *Rc*mini23S antisense, 5′-GGGGGAAGCTTGTTGACTCATGTCAACATTCTC-3′ (30 nt, *Hin*dIII site underlined). Primers for amplification of the *E.coli* mini substrate DNA using *E.coli* chromosomal DNA as template were: *Ec*mini23S sense, 5′-GGGGGGAATTCTAATACGACTCACTATAGGTTCTGTAAGCCTGCGAAGGTG TGCTGT-3′ (57 nt, *Eco*RI site underlined); *Ec*mini23S antisense, 5′-GGGGGAAGCTTGCTGACTTATGTCAGCATTCGC-3′ (33 nt, *Hin*dIII site underlined). The 5′ sense primers carry a T7 promoter region for transcription initiation. PCR was carried out at annealing temperatures of 45°C (45 s), followed by extension at 72°C (30 s). Cycles were repeated 31 times. The resulting PCR products were purified from low melting point agarose gels. Finally, the particular PCR products were cut with *Hin*dIII and *Eco*RI and cloned into pUC18 vectors. Integrity of the insert was confirmed by sequencing of the resulting plasmids.

In vitro transcription of RNAs

The pUC18 vector templates for *in vitro* transcription carrying the DNA sequence of the particular RNA substrate located behind a T7 promoter were linearized with *Hin*dIII (for *Rc* and *Ec* mini RNAs, respectively) or *Hpa*II (*Hpa* mini RNA) to enable run-off transcription. As templates for N26 and N44 we used oligonucleotides with an annealed 18mer promoter oligonucleotide (24,25). *In vitro* transcription with T7 RNA polymerase (NEB) was performed as described elsewhere (23,26). To generate internally labelled RNAs, [α-^{32}P]UTP (20 µCi) was included in each transcription reaction. Polynucleotide kinase (PNK) was used for 5′-labelling of dephosphorylated RNAs, with 50 µCi [α-^{32}P]ATP per reaction added. Radioactively labelled RNA transcripts were purified on a 10% polyacrylamide–7 M urea gel, the bands cut out and the substrates eluted from the crushed gel bands overnight at room temperature in RNA elution buffer (0.5 M NaOAc, pH 5.0, 1 mM EDTA, pH 8.0, 2.5% v/v phenol). Specific activities of the RNAs were of the order of 10^5 c.p.m./pmol.

Enzymatic assays

In addition to the *Rc*, *Hpa* and *Ec* mini RNAs, two variants of the well-studied phage T7 R1.1 processing signal for RNase III, N26 and N44, were used as substrates (Fig. 1). The latter have been described elsewhere (24,25). Cleavage assays were performed using *in vitro* transcribed RNA substrates, either internally labelled or 5′-labelled as described above. The assays were carried out in cleavage buffer (30 mM Tris–HCl, pH 7.5, 10 mM $MgCl_2$ or MgOAc, 130 mM KCl, 5% glycerol) at 37 or 32°C for the indicated time (usually 1–3 min). In some assays monovalent cations were omitted to determine their influence on cleavage specificity of RNase III. For each assay 5000 c.p.m. of the particular substrate were used. Assay volumes were 10 µl. The reactions were stopped by addition of 8 µl formamide-containing dye and placed on ice. Reaction products were incubated at 65°C for 3 min and analysed on a 10% polyacrylamide–7 M urea gel. Bands were detected by autoradiography.

Mapping of the RNase III cleavage site by primer extension

To determine the position of the RNase III processing site in the *Rc* mini RNA we used primer extension analysis. The primer for the extension reaction (*Rc*mini ext) had the sequence 5′-CGCTTCTGATCACTCCAC-3′ and annealed to nt 96–113 of

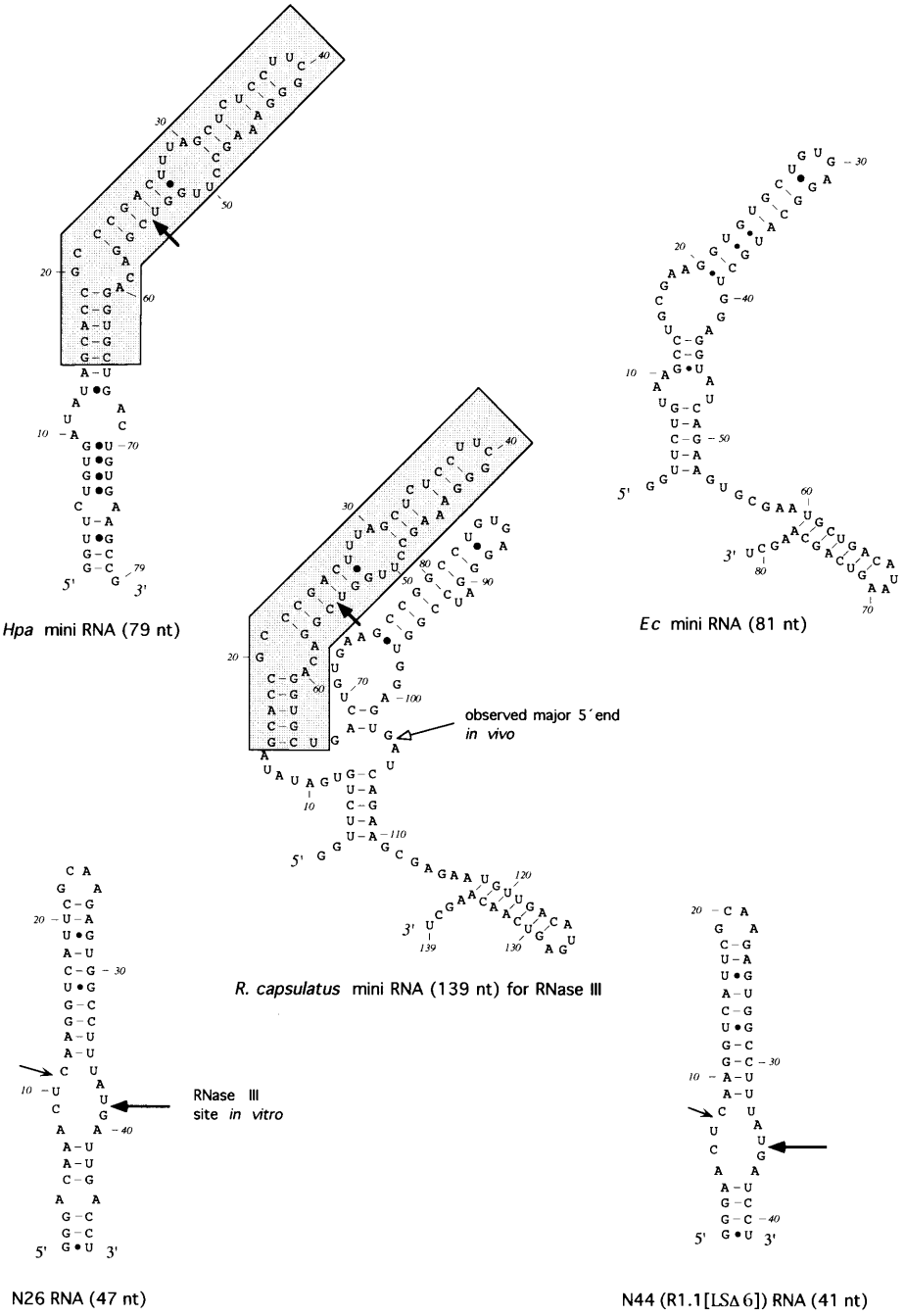

substrate	*Rc* mini RNA	*Hpa* mini RNA	*Ec* mini RNA	N26 RNA	N44 RNA
length [nt]	139	79	81	47	41
fragments generated: ➡ primary site	54[5']+85[3']	54[5']+25[3']	no cleavage	38[5']+9[3']	35[5']+6[3']
→ secondary site	—	—	no cleavage	38 [5']⇨28+10	35 [5']⇨28+7

Figure 1. Proposed secondary structures of the RNA substrates for RNase III used in this study. The processing sites for RNase III are indicated by arrows: bold arrows, primary site; small arrow, secondary site. Shaded boxes highlight the *R.capsulatus* extra stem–loop element in the *Rc* mini and *Hpa* mini RNAs. The table summarizes the fragment sizes resulting from *Rhodobacter* RNase III cleavage at primary and secondary sites, respectively.

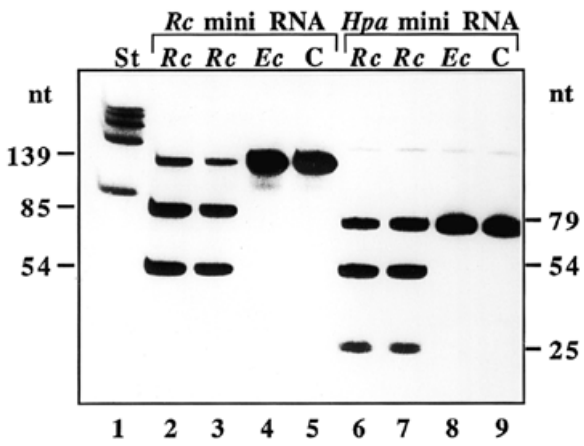

Figure 2. Processing of 139 nt *Rc* mini and 79 nt *Hpa* mini substrate (2000 c.p.m./lane) by *R.capsulatus* (*Rc*) and *E.coli* (*Ec*) RNase III (30 nM dimer) in standard cleavage buffer (Materials and Methods). St, RNA standard (500–100 nt); C, control.

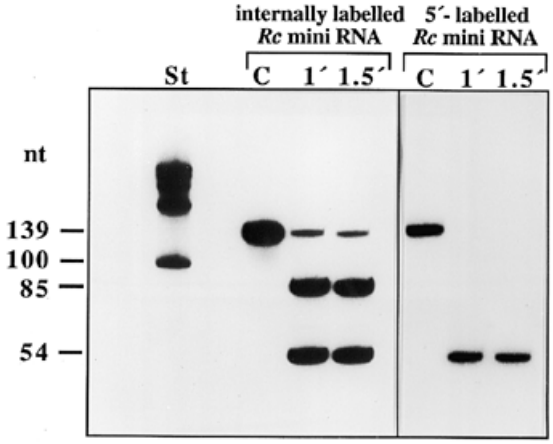

Figure 3. Cleavage of internally and 5′-labelled *Rc* mini RNA (~3000 c.p.m./lane) by *R.capsulatus* RNase III (30 nM dimer) in standard cleavage buffer. 1′ and 1.5′, incubation of *Rc* mini RNA with *R.capsulatus* RNase III for 1 and 1.5 min, respectively.

the *Rc* mini RNA (see Fig. 1). Aliquots of 100 pmol primer were labelled for 30 min at 37°C with 30 µCi [γ-^{32}P]ATP using polynucleotide kinase and subsequently purified with a NucTrap® push column (Stratagene). Unlabelled *Rc* mini substrate RNA was incubated with *R.capsulatus* $(His)_6$-RNase III (30 nM dimer) in cleavage buffer at 37°C for 5, 10 or 15 min. After phenol extraction and ethanol precipitation of the RNA the substrate was dissolved in 5 µl 2× primer extension buffer (100 mM Tris–HCl, pH 8.3, 100 mM KCl, 20 mM $MgCl_2$, 20 mM DTT, 0.2 mM spermidine, 2 mM each dNTPs). Approximately 200 000 c.p.m. primer and 5 µg *E.coli* tRNA were added and annealing took place in a final volume of 10 µl for 10 min at 70°C. The samples were cooled to room temperature and another 5 µl 2× primer extension buffer, 1.4 µl 40 mM sodium pyrophosphate, 2.6 µl water and 1 µl AMV reverse transcriptase (23 U/µl) were added. The reaction was incubated for 30 min at 42°C and precipitated with isopropanol at room temperature. The precipitate was dissolved in water, heated (10 min, 90°C) and analysed on a polyacrylamide–urea gel. Sequencing reactions of the DNA template for the *Rc* mini substrate using the same primer were loaded on the same gel to map the position of the cleavage site for RNase III.

Immunological methods

Anti-RNase III sera directed against *E.coli* and *R.capsulatus* RNase III, respectively, were raised using *E.coli* RNase III, purified via poly(I)·poly(C) affinity chromatography (24), and *R. capsulatus* $(His)_6$-RNase III, purified using Ni-NTA chromatography, as antigens. The purified proteins were lyophilized and used for production of antibodies in rabbits (Eurogentech, Belgium). Sera were purified using protein A–Sepharose chromatography. For western blot analysis, proteins were separated by SDS–PAGE on 15% polyacrylamide gels and transferred to nitrocellulose by semi-dry electroblotting (Pharmacia). Membranes were incubated with anti-RNase III antibodies (1:200) or corresponding pre-immune sera as a control. Immune complexes were detected with anti-rabbit IgG alkaline phosphatase conjugate (diluted 1:7000; Sigma) and nitroblue tetrazolium (NBT)/BCIP (X-phosphate) as substrate for the colour reaction.

Gel electrophoretic mobility shift assay

To detect formation of RNA–RNase III complexes, [α-^{32}P]UTP-labelled *Rc* mini substrate (10 000 c.p.m.) was dissolved in 2× shift buffer (320 mM KCl, 60 mM Tris–HCl, pH 7.5, 10 mM EDTA, 20% v/v glycerol, 0.2 mM DTT) and incubated with various amounts of *R.capsulatus* or *E.coli* RNase III for 1 h at room temperature. The samples were then placed on ice. Aliquots were run on 7% polyacrylamide gels containing 0.5× TBE buffer for ~4 h at 10 V/cm in a cold room. The gels were dried and radioactive bands were detected by autoradiography.

RESULTS

Purification of *R.capsulatus* RNase III

$(His)_6$-RNase III from *R.capsulatus* was purified to apparent homogeneity using Ni-NTA affinity chromatography. We were able to isolate ~15–20 mg recombinant RNase III from 1.4 g *E.coli* M15 cells. During 2 h bacterial growth after IPTG induction and increased production of recombinant RNase III a toxic effect on the cells was not observed. A mock purification of IPTG-induced M15 cells carrying the pQE vector without the *rnc* insert showed no RNase III-like activity in the enzymatic assay (data not shown). This indicates that endogenous RNase III of *E.coli* M15 did not bind to the Ni-NTA column. The enzymatic activity observed is therefore due to $(His)_6$-RNase III of *R.capsulatus* only.

Biochemical properties of $(His)_6$-RNase III

To study the biochemical properties of *R.capsulatus* RNase III, we tested the enzyme's dependence on divalent cations and the influence of monovalent cations on cleavage of additional sites in the employed RNA substrates (*Rc* mini, *Hpa* mini, *Ec* mini, N26 and N44; Fig. 1). These substrates are either derived from 23S rRNA structures of *R.capsulatus* (*Rc* and *Hpa* mini substrates) or

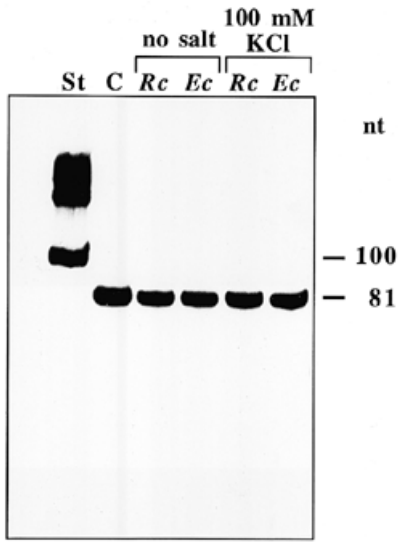

Figure 4. Incubation of *Ec* mini RNA (3000 c.p.m./assay) with *R.capsulatus* (*Rc*) and *E.coli* (*Ec*) RNase III (30 nM dimer) at different salt concentrations.

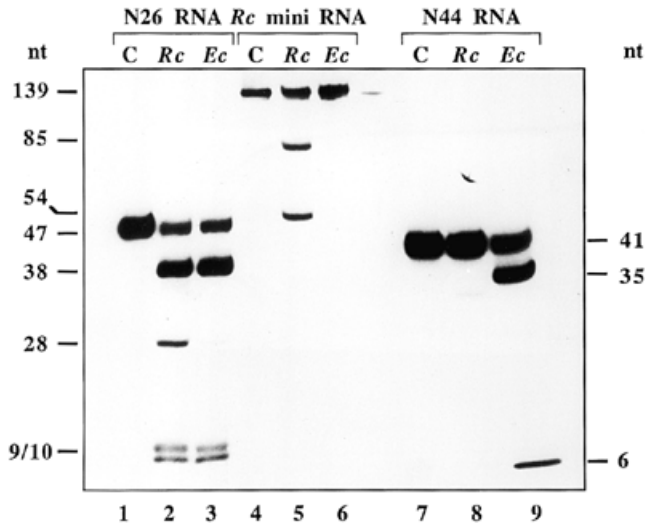

Figure 5. Three different RNA substrates (N26, *Rc* mini, N44; 2000 c.p.m./lane each) incubated for 3 min at 37°C with *R.capsulatus* (*Rc*) or *E.coli* (*Ec*) RNase III (30 nM dimer) in standard assay buffer. C, control.

E.coli (*Ec* mini), respectively, or from the phage T7 R1.1 RNase III processing signal (N26 and N44). Maximum activity of the enzyme was observed at a pH of 7.5 (32°C) with 10–20 mM $MgCl_2$ using N26 RNA as a substrate. Mn^{2+} and Co^{2+} can substitute for Mg^{2+} (optima at 1 and 5 mM, respectively), whereas Ca^{2+} and Zn^{2+} (0–50 mM) do not support enzymatic activity (data not shown). Thus *Rhodobacter* RNase III has the same divalent cation requirements as *E.coli* RNase III, with only slightly different optima. Recombinant RNase III from *R.capsulatus* and wild-type *Rhodobacter* RNase III, which had been partially purified using ion exchange chromatography, show the same substrate specificity with the N26 RNA (data not shown). Catalytic activity of RNase III is not inhibited by 40 U RNasin® RNase inhibitor (Promega). The ion requirements of *R.capsulatus* RNase III resemble those of *E.coli* RNase III, although with somewhat altered optima.

Substrate specificity

To address the special situation of fragmented 23S rRNA in *Rhodobacter* we used *in vitro* substrates derived from the extended helix 46 processing site of RNase III in *R.capsulatus* rRNA. The corresponding canonical stem–loop 46 of *E.coli*, the recipient site for the extra stem–loop, served as an additional *in vitro* substrate which, though also structured, is not cleaved by RNase III (*Ec* mini RNA). The two *Rhodobacter* mini 23S rRNA substrates we designed (Fig. 1) are processed *in vitro* by RNase III of *R.capsulatus* while purified *E.coli* RNase III shows no detectable enzymatic activity with the same substrates under identical conditions. With the *Rc* mini RNA (139 nt) the resulting fragments are 54 and 85 nt in size; the smaller *Hpa* mini substrate (79 nt) is cleaved into fragments of 54 and 25 nt (Fig. 2). In each case the 54 nt fragment carries the 5′-end of the molecule, as demonstrated by cleavage of the 5′-labelled substrates and comparison of the resulting fragment(s) with the products resulting from cleavage of the internally labelled substrates (Fig. 3).

In contrast, the RNA substrate containing just *E.coli* rRNA helix 46 (*Ec* mini RNA, 81 nt; Fig. 1) is not processed by RNase III from *R.capsulatus* or *E.coli* even at low concentrations of monovalent cations (Fig. 4). It has been noted before that otherwise unreactive RNAs could serve as RNase III substrates at low salt concentrations (27–29).

N26 RNA (47 nt) derived from the R1.1 processing signal is processed by both enzymes in a similar manner (Fig. 5). The cleavage specificity of *R.capsulatus* RNase III is influenced by the concentration of monovalent cations: a secondary site is cleaved (in addition to the primary processing site) at low salt concentrations (see Fig. 1). This was previously noted for *E.coli* RNase III (24). *Rhodobacter* RNase III exhibits a stronger preference for the secondary cleavage site of the N26 substrate than does the *E.coli* enzyme (Fig. 5, lanes 2 and 3). In cleavage of N26 RNA the 9/10 nt doublet band is due to non-template-directed addition of a nucleotide to the 3′-terminus of the nascent transcript by T7 RNA polymerase (26,27). An additional 10 nt band (carrying the N26 5′-end) resulting from cleavage at the secondary site contains only one ^{32}P-labelled uridine residue and therefore does not significantly increase the signal of the 10 nt band resulting from the heterogeneous 3′-end. The *Rc* mini RNA shows secondary site cleavage at low concentrations of monovalent cations (Fig. 6, lane 3), resembling R1.1-derived substrates (24,28,29). The slightly shorter N44 RNA (41 nt) cannot be cleaved by RNase III of *R.capsulatus* under conditions where cleavage by *E.coli* RNase III occurs (Fig. 5, lanes 8 and 9). In the absence of NH_4Cl the enzymes of both organisms are able to process the *R.capsulatus* 139 nt mini substrate (Fig. 6, lanes 3 and 4). At concentrations of 100 mM KCl or NH_4Cl, however, RNase III of *R.capsulatus* exhibits normal processing activity with the *Rc* mini RNA whereas the *E.coli* enzyme no longer cleaves the substrate. Processing activity of the *R.capsulatus* enzyme significantly decreases at salt concentrations higher than 150 mM KCl. At concentrations of >200 mM KCl or NH_4Cl *Rhodobacter* RNase III no longer cleaves the mini substrate (Fig. 6).

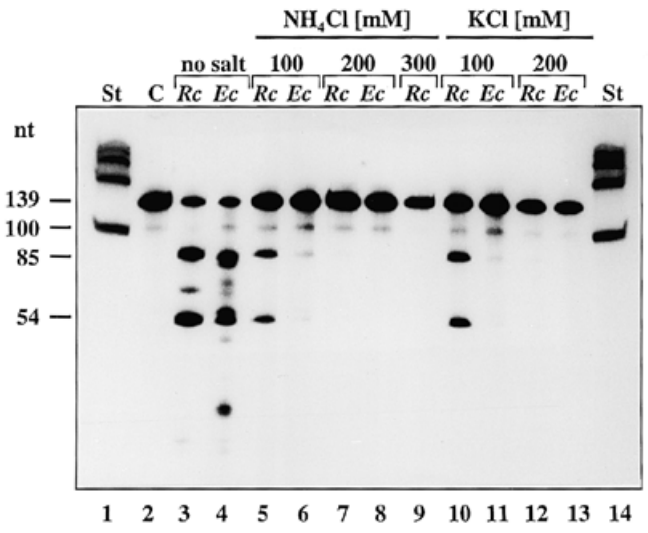

Figure 6. Processing of 139 nt *Rc* mini RNA (2000 c.p.m./lane) by *R.capsulatus* (*Rc*) and *E.coli* (*Ec*) RNase III (30 nM dimer) at different concentrations of monovalent cations. Standard cleavage buffer without salt was supplemented with NH_4Cl and KCl, respectively. C, uncleaved substrate; St, RNA standard (500–100 nt).

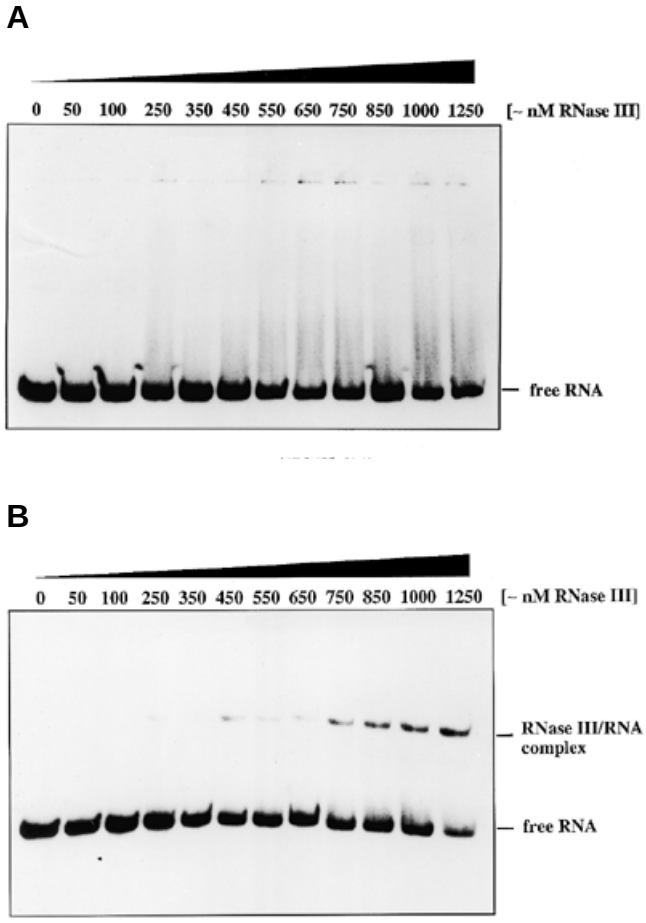

Figure 7. (**A**) Gel mobility shift assay with *E.coli* RNase III and *Rc* mini RNA (10 000 c.p.m./lane). (**B**) Gel mobility shift assay with *R.capsulatus* RNase III and *Rc* mini substrate (10 000 c.p.m./lane). A shifted complex becomes visible at ~250 nM RNase III.

Binding of RNase III to *Rc* mini RNA

To examine whether the extremely reduced processing activity of *E.coli* RNase III with the 139 nt *Rc* mini RNA (see above) is due to lack of substrate binding or due to impaired enzymatic catalysis we employed gel shift experiments. Gel electrophoretic mobility shift assays under identical binding conditions show a higher affinity of *R.capsulatus* RNase III for *Rc* mini RNA compared with RNase III from *E.coli* (Fig. 7A and B). *Escherichia coli* RNase III is apparently unable to bind the *Rc* mini substrate with an affinity as high as the *R.capsulatus* enzyme. This corresponds to the lower processing activity of *E.coli* RNase III with the *Rc* mini substrate compared with the *R.capsulatus* enzyme (Figs 5 and 6).

Position of the cleavage site for RNase III in the *Rc* mini RNA

Previous experiments (8) using low resolution primer extension and oligonucleotide probing indicated the presence of an *in vivo* processing site for RNase III in *Rhodobacter* rRNA at position 1364 of the large ribosomal subunit RNA (numbering according to the rRNA database entry). In addition to this major 5′-end of the RNA fragment (indicated in Fig. 1), a minor 5′-end at position 1321 was observed (nt 57 in *Rc* mini RNA; Fig. 1). Both 5′-ends were thought to be generated by RNase III cleavage. Alternatively, the major 5′-end could arise from subsequent exonucleolytic processing after cleavage at the observed minor 5′-end. Our primer extension analysis of the cleaved *Rc* mini RNA shows that the *in vitro* processing site appears to be exclusively located between nucleotides U54 and C55 (Fig. 8; 1). In this region the RNA is predicted to be double-stranded. The double-stranded region with the cleavage site is flanked by bulge loops on both sides, resembling a ‘bulge–helix–bulge’ motif. The position of this site is very close to the previously described *in vivo* minor 5′-end. The observed major 5′-end *in vivo* must originate from subsequent trimming of the 3′-fragment after an initial cut at U54.

Immunological behaviour of RNase III

Despite strong sequence similarity of *R.capsulatus* and *E.coli* RNases III polyclonal antibodies raised against the *E.coli* enzyme do not crossreact with the $(His)_6$-tagged enzyme from *Rhodobacter*. A polyclonal antiserum against the His-tagged enzyme of *R.capsulatus* does not show crossreaction with purified RNase III of *E.coli* during western blot analysis (Fig. 9).

DISCUSSION

As a starting point for an analysis of the interaction of *Rhodobacter* RNase III with the 23S rRNA fragmentation site we first chose cleavage reactions with two well-established substrates used during analysis of *E.coli* RNase III, N26 and N44 (see Fig. 1). Both substrates are related to the T7 phage early RNA R1.1 processing site (28). The N26 substrate has 47 nt comprising the stem–loop of the original R1.1 site. An upper and lower helical stem are connected through an asymmetrical internal loop. For substrate recognition *E.coli* RNase III does not require the internal loop and terminal tetraloop found in N26 (27). This substrate is readily processed by RNase III of *E.coli* and has since

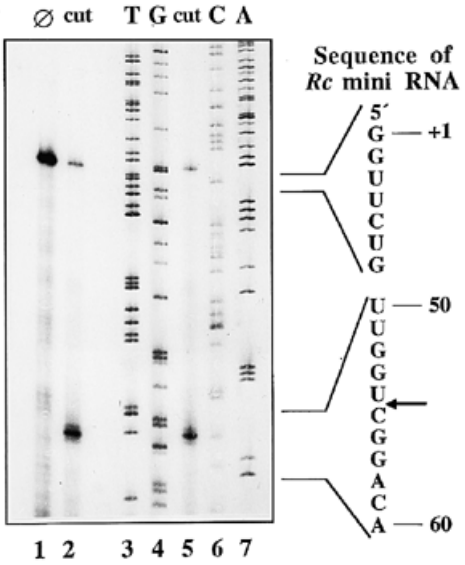

Figure 8. Primer extension analysis of *Rc* mini RNA cleaved by *R.capsulatus* RNase III. Ø (lane1), 5′-end of the uncleaved *Rc* mini RNA; cut (lanes 2 and 5), observed 5′-ends after cleavage of the RNA substrate by *R.capsulatus* RNase III (5 min, 37°C). The upper band corresponds to the 5′-end of the full-length substrate (compare lane 1). The lower band indicates the additional 5′-end after RNase III cleavage of the *Rc* mini RNA. The 5′-end of this band corresponds to C54 (compare lanes 5 and 6 and Fig. 1). T, G, C, A (lanes 3, 4, 6 and 7), each letter refers to the corresponding nucleotide of the *Rc* mini DNA template as determined by dideoxy sequencing. Parts of the *Rc* mini RNA sequence are indicated on the right side of the figure and are numbered according to Figure 1. The RNase III cleavage site has been marked by an arrow.

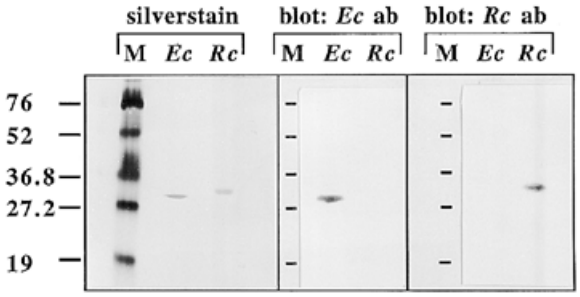

Figure 9. Immunocrossreactivity of *R.capsulatus* (*Rc*) and *E.coli* (*Ec*) RNases III (2 µg). The left panel shows a silver stained SDS–PAGE gel with both enzymes. The two right hand panels show western blots of this gel incubated with antibodies (ab) against *E.coli* RNase III (*Ec* ab) and *R.capsulatus* (*Rc* ab) RNase III, respectively. M, protein standard (BioRad), molecular weight indicated in kDa.

been the standard for RNase III activity assays. A single nucleotide bond located in the internal loop is cut under standard conditions. When assayed with *Rhodobacter* RNase III under identical conditions the enzyme shows optimal ion requirements comparable with those of *E.coli* RNase III (24). The preferred divalent cation is Mg^{2+} at a concentration of 10–20 mM, with Mn^{2+} and Co^{2+} able to substitute at optimal concentrations of 1 and 5 mM, respectively. Ca^{2+} and Zn^{2+} do not support catalytic activity. Me^{2+} ions are important for catalysis but their impact in substrate recognition appears to be rather limited. Protein contact appears to be established through direct sugar–phosphate backbone interaction (30). As with *E.coli* RNase III, substitution with Mn^{2+} and Co^{2+} significantly increases processing at an otherwise dormant secondary cleavage site in the loop (24). This is also the case when the concentration of monovalent cations is lowered. In summary, *Rhodobacter* RNase III performs very similarly to the *E.coli* enzyme when assayed with N26 RNA.

N44 is derived from N26 with a shorter helix by just 3 bp. Structural analysis of N44 by NMR spectroscopy, optical melting and chemical and enzymatic modification showed that it retains all the structural features of the parent molecule N26 (25). It also resembles N26 with respect to primary and secondary site cleavage and is readily processed by *E.coli* RNase III with only slightly reduced reactivity (25,27). Under standard salt concentrations we could not detect cleavage of N44 RNA by *Rhodobacter* RNase III (Fig. 5, lane 8). With just 3 bp less a critical threshold value for helix length is obviously no longer met by this substrate. At low salt conditions, the N44 RNA is cleaved by RNases III of both organisms (not shown). We noticed that a single-stranded extension of the N44 3′-end by just 4 nt (5′-ACCA-3′) (N44+4) restored cleavage in this substrate. To determine the contribution of the additional nucleotides we constructed three RNAs extended by 1, 2 or 3 nt at the 3′-end. The nucleotides used for the extensions were A (N44+1), AC (N44+2) and ACC (N44+3). Instead of the G·U base pair at the termini of the N44 RNA lower stem (Fig. 1) all of the extended substrates possess an A instead of the terminal 3′ U, therefore lacking this G·U interaction. The 1 nt (A) extension does not restore substrate character to N44 RNA. Cleavage of N44 RNA seems to be restored by the addition of 2 nt (AC). N44+3 (ACC) RNA, however, is processed with a slightly reduced activity. Although increased processing is observed through the mere addition of 3′ nucleotides, further experiments are necessary for a detailed analysis of the contribution of the lower stem.

We then analysed substrates derived from the fragmentation site in *Rhodobacter* 23S rRNA. The 139 nt *Rc* mini RNA (Fig. 1) comprises the canonical helix 46 and the inserted extra stem–loop. *Rhodobacter* RNase III cleaves this substrate exclusively at the nucleotide bond between U54 and C55 (Figs 2 and 8). The position of the cleavage site was confirmed by primer extension of the 3′ cleavage product (Fig. 8) and by using 5′-labelled *Rc* mini substrate (Fig. 3). The site thus corresponds well to the previously observed minor 5′-end *in vivo* (8). An alternative way of processing this substrate would be cleavage of a dormant RNase III site in the canonical stem, possibly unmasked through structural changes after insertion of the extra stem–loop. We excluded cleavage in the canonical stem–loop by constructing a substrate which comprises the *E.coli* stem–loop alone (*E.coli* mini RNA; Fig. 1). This stem–loop is highly similar in *E.coli* and *Rhodobacter.* Neither *Rhodobacter* nor *E.coli* RNase III could process this substrate (Fig. 4). The observed major 5′-end generated *in vivo* after fragmentation lies ~50 nt downstream of the minor 5′-end, well within helix 46 (Fig. 1; 8). To explain this fact, either the action of a second endonuclease or the presence of a 5′→3′ exonuclease would have to be postulated. This exonuclease type has not been described yet in bacteria.

Surprisingly, *E.coli* RNase III does not cleave the 139 nt *Rc* mini RNA. This indicates that the *Rhodobacter* mini substrate must have clear structural deviations from the standard *E.coli*

substrate type. The dsRBD of *Rhodobacter* RNase III must be structurally adapted to these changes.

To provide more evidence for the 'plug-in' character of the extra stem–loop conferring cleavage at the insertion site, we constructed the 79 nt *Hpa* mini RNA (Fig. 1) taking advantage of a naturally occurring *Hpa*I site. This substrate comprises only the extra stem–loop with some additional terminal base pairs. This substrate is also precisely cleaved by *Rhodobacter* RNase III at position U54, but again is not cleaved by the *E.coli* enzyme (Fig. 2, lane 8). These results are in line with recent experiments where RNase III cleavage was conferred by introducing an RNase III-cleavable element into phage RNA genomes (31) or into a site in *E.coli* 23S rRNA. In the latter case a *Salmonella* spp. RNase III element from helix 45 of *Salmonella* 23S rRNA was introduced into helix 45 of unfragmented *E.coli* 23S rRNA, a site in close proximity to the *Rhodobacter* helix 46 (32). Interestingly, in this experiment the transferred *Salmonella* RNA element could be processed by RNase III from *E.coli* leading to a fragmented *E.coli* 23S rRNA, whereas the *Rhodobacter* element cannot be processed, at least not *in vitro*. The area around helix 46 makes only limited protein contacts in the ribosome and is exposed to the surface at the back of the central body of the large subunit (R.Brimacombe, personal communication). This is possibly important for processing of the 23S rRNA at a specific point in ribosome assembly.

The complex between the *Rhodobacter* 23S-derived substrate and RNase III appears to be particularly strong. The complex between N26 substrate and *E.coli* RNase III is unstable in non-denaturing gels. Only a fully base paired substrate variant provides stable complexes. This stability is then accompanied, though, by increased second site cleavage of the base paired substrate (27). The internal loop secures single site cleavage at the expense of higher instability of the enzyme–substrate complex. In our shift experiments under comparable conditions *E.coli* RNase III does not bind the *Rhodobacter* mini substrate (Fig. 7A). *Rhodobacter* RNase III instead forms a stable complex with this substrate (Fig. 7B), even in the absence of Mg^{2+}, which is known to stabilize RNase III–substrate complexes (27). Formation of a stable complex and single site cleavage in this case do not exclude each other.

What structural features mark the differences between *Rhodobacter* and *E.coli* dsRBDs? The assumption that structural differences exist is supported by the observation that *Rhodobacter* RNase III does not bind to poly(I)·poly(C) resins under standard affinity chromatography conditions described for *E.coli* RNase III (24; data not shown). Furthermore, the mutual lack of antibody recognition between RNases III from *E.coli* and *R.capsulatus* points in that direction. The *Rhodobacter* dsRBD fits the general α-β-β-β-α structure of a dsRBD as described for the dsRBDs of *Drosophila* Staufen protein and RNase III from *E.coli* (33,34). Two α-helices are positioned against the backdrop of a three-stranded antiparallel β-sheet. The amino acid sequences of the *Rhodobacter* and *E.coli* dsRBD, though not identical, show strong homology with the consensus sequence for dsRBDs (20).

We have identified a new RNA element which confers fragmentation on *Rhodobacter* 23S rRNA. It remains to be seen whether substrate recognition is dependent exclusively on recognition by a rigid dsRBD or whether it relies on a more subtle adaptive binding to the dsRBD and presentation of the substrate to the catalytic centre in the N-terminal half of the enzyme.

ACKNOWLEDGEMENTS

The templates for the N26 and N44 substrates and the *E.coli* strain HMS174(DE3)/pET-11a(*rnc*) were a generous gift of A.W.Nicholson (Detroit). The authors would like to thank Stephanie Schmalz and Christoph Scherfer for their assistance. This work was supported by Fonds der Chemischen Industrie.

REFERENCES

1 Bram,R., Young,R. and Steitz,J. (1980) *Cell*, **19**, 393–401.
2 Abou Elela,S., Igel,H. and Ares,M.,Jr (1996) *Cell*, **85**, 115–124.
3 Nicholson,A.W. (1996) *Prog. Nucleic Acid Res. Mol. Biol.*, **52**, 1–65.
4 Dunn,J.J. (1982) In Boyer,P.D. (ed.), *The Enzymes*, Vol. XV, *Nucleic Acids*, Part B. Academic Press, New York, NY, pp. 485–499.
5 Chen,S.-M., Takiff,H.E., Barber,A.M., Dubois,G.C., Bardwell,J.C.A. and Court,D.L. (1990) *J. Biol. Chem.*, **265**, 2888–2895.
6 Babitzke,P., Granger,L., Olszewski,J. and Kushner,S.R. (1993) *J. Bacteriol.*, **175**, 229–239.
7 Fraser,C.M., Gocayne,J.D., White,O., Adams,M.D., Clayton,R.A., Fleishmann,R.D., Bult,C.J., Kerlavage,A.R., Sutton,G., Kelley,J.M. *et al.* (1995) *Science*, **270**, 397–403.
8 Kordes,E., Jock,S., Fritsch,J., Bosch,F. and Klug,G. (1994) *J. Bacteriol.*, **176**, 1121–1127.
9 Burgin,A.B. Parodos,K., Lane,D.J. and Pace,N.R. (1990) *Cell*, **60**, 404–414.
10 Winkler,M.E. (1979) *J. Bacteriol.*, **139**, 842–849.
11 Doolittle,W.F. (1973) *J. Bacteriol.*, **113**, 1256–1263.
12 Schuch,W. and Loening,U.E. (1975) *Biochem. J.*, **149**, 17–22.
13 Marrs,B.L. and Kaplan,S. (1970) *J. Mol. Biol.*, **49**, 297–317.
14 Gray,M.W. and Schnare,M.N. (1996) In Zimmermann,R.A. and Dahlberg,A.E. (eds), *Ribosomal RNA*. CRC Press, Boca Raton, FL, pp. 49–69.
15 Hsu,D., Shih,L.-M. and Zee,Y.C. (1994) *J. Bacteriol.*, **176**, 4761–4765.
16 Dam,M., Douthwaite,S., Tenson,T. and Mankin,A.S. (1996) *J. Mol. Biol.*, **256**, 1–6.
17 Rotondo,G. and Frendewey,D. (1996) *Nucleic Acids Res.*, **24**, 2377–2386.
18 Saks,M.E., Sampson,J.R. and Abelson,J.N. (1994) *Science*, **263**, 191–197.
19 Zhang,K. and Nicholson,A.W. (1997) *Proc. Natl Acad. Sci. USA*, **94**, 13437–13441.
20 Burd,C.G. and Dreyfuss,G. (1994) *Science*, **265**, 615–621.
21 St Johnston,D., Brown,N.H., Gall,J.G. and Jantsch,M. (1991) *Proc. Natl Acad. Sci. USA*, **89**, 10979–10983.
22 Schmedt,C., Green,S.R., Manche,L., Taylor,D.R., Ma,Y. and Mathews,M.B. (1995) *J. Mol. Biol.*, **249**, 29–44.
23 Rauhut,R., Jäger,A., Conrad,C. and Klug,G. (1996) *Nucleic Acids Res.*, **24**, 1246–1251.
24 Li,H.-L., Chelladurai,B.S., Zhang,K. and Nicholson,A.W. (1993) *Nucleic Acids Res.*, **21**, 1919–1925.
25 Schweisguth,D.C., Chelladurai,B.S., Nicholson,A.W. and Moore,P.B. (1994) *Nucleic Acids Res.*, **22**, 604–612.
26 Milligan,J.F., Groebe,D.R., Witherell,G.W. and Uhlenbeck,O.C. (1987) *Nucleic Acids Res.*, **14**, 8783–8798.
27 Chelladurai,B.S., Li,H., Zhang,K. and Nicholson,A.W. (1993) *Biochemistry*, **32**, 7549–7558.
28 Dunn,J.J. (1976) *J. Biol. Chem.*, **251**, 3807–3814.
29 Gross,G. and Dunn,J.J. (1987) *Nucleic Acids Res.*, **15**, 431–442.
30 Li,H. and Nicholson,A. W (1996) *EMBO J.*, **15**, 1421–1433.
31 Klovins,J., van Duin,J. and Olsthoorn,R.C.L. (1997) *Nucleic Acids Res.*, **25**, 4201–4208.
32 Gregory,S.T., O'Connor,M. and Dahlberg,A.E. (1996) *Nucleic Acids Res.*, **24**, 4918–4923.
33 Bycroft,M., Grünert,S., Murzin,A.G., Proctor,M. and St Johnston,D. (1995) *EMBO J.*, **14**, 3563–3571.
34 Kharrat,A., Macias,J., Gibson,T.J., Nilges,M. and Pastore,A. (1995) *EMBO J.*, **14**, 3572–3584.